Hydrogen Evolution Reaction

Deutsche Ausgabe: DOI: 10.1002/ange.201411450
Internationale Ausgabe: DOI: 10.1002/anie.201411450

Single-Shell Carbon-Encapsulated Iron Nanoparticles: Synthesis and High Electrocatalytic Activity for Hydrogen Evolution Reaction**

*Mohammad Tavakkoli, Tanja Kallio, Olivier Reynaud, Albert G. Nasibulin, Christoffer Johans, Jani Sainio, Hua Jiang, Esko I. Kauppinen, and Kari Laasonen**

Abstract: *Efficient hydrogen evolution reaction (HER) through effective and inexpensive electrocatalysts is a valuable approach for clean and renewable energy systems. Here, single-shell carbon-encapsulated iron nanoparticles (SCEINs) decorated on single-walled carbon nanotubes (SWNTs) are introduced as a novel highly active and durable non-noble-metal catalyst for the HER. This catalyst exhibits catalytic properties superior to previously studied nonprecious materials and comparable to those of platinum. The SCEIN/SWNT is synthesized by a novel fast and low-cost aerosol chemical vapor deposition method in a one-step synthesis. In SCEINs the single carbon layer does not prevent desired access of the reactants to the vicinity of the iron nanoparticles but protects the active metallic core from oxidation. This finding opens new avenues for utilizing active transition metals such as iron in a wide range of applications.*

Progress in hydrogen economy and utilization of hydrogen as a future energy carrier will require sustainable, efficient, and cost-effective production of hydrogen.[1] Among current technologies for H_2 production, water splitting (i.e., $H_2O \rightarrow H_2 + {}^1/_2 O_2$) is one of the most attractive and simple methods to produce hydrogen. Electrochemical water splitting is divided into two half reactions: the hydrogen evolution reaction (HER, $2H^+ + 2e^- \rightarrow H_2$) and the oxygen evolution reaction (OER, $H_2O \rightarrow 2H^+ + 2e^- + {}^1/_2 O_2$).[2] For HER, platinum-based catalysts are currently the most efficient electrocatalysts with an onset overpotential (η) close to zero; however, the high cost and scarcity of platinum limit its large-scale commercial application.[3] Therefore, low-cost, efficient, and stable non-noble-metal catalysts for HER are required, especially for acidic media because of the strongly acidic conditions met in devices based on proton exchange membrane technology.[4] In the past decade, many researches have been devoted to introduce efficient non-noble-metal catalysts for HER. Recent advances have been reported for molybdenum-based compounds,[5] Co-based compounds,[4,6] Ni_2P,[7] a FeCo alloy encapsulated in nitrogen-doped carbon nanotubes (NCNTs),[8] FeP–graphene sheets,[9] a C_3N_4@nitrogen-doped graphene hybrid,[10] and nitrogen and phosphorus dual-doped graphene.[11]

Metal nanoparticles encapsulated in carbon cages are promising highly active nanostructures with high chemical and thermal stability, because the encapsulating shell protects the metal nanoparticle from atmospheric-oxygen-induced degradation and agglomeration of neighboring nanoparticles. Thus, these new structures enable technological applications of metal nanoparticles as the naked ones are not stable enough in ambient air.[12] Few-shell carbon-encapsulated metal nanoparticles have been found to catalyze the oxygen reduction reaction (ORR)[12] and HER.[6,8] A high catalytic activity towards ORR is also reported for iron carbide nanoparticles encased in graphitic layers.[13] However, in these structures, the multiple layers of carbon covering the particles hinder desired access of the reactants to the vicinity of the iron nanoparticle and therefore the catalytic activity of the metal is significantly decreased. To our knowledge, single-shell carbon-encapsulated metal nanoparticles (SCEINs) have not been experimentally reported earlier. However, they were recently studied with density functional theory (DFT) and a considerable charge transfer from iron to carbon was reported, inducing active sites for catalysis in these materials.[14]

The unique structure and intrinsic properties of carbon nanotubes such as high surface area, high chemical stability, high electrical conductivity, and insolubility in most solvents, make them extremely attractive as supports for heterogeneous catalysts.[3a,4,5f,15] Thus, the growth of nanoparticles supported on carbon nanotubes is an interesting approach to create efficient catalysts. In this study, we focused on the growth of SCEINs decorated on single-walled carbon nanotubes (SWNTs) to obtain the desired catalytic activity for HER. Moreover, we used a low-cost chemical vapor deposition (CVD) method in which both the catalyst (SCEIN) and the support (SWNT) were synthesized simultaneously; this

[*] M. Tavakkoli, Dr. T. Kallio, Dr. C. Johans, Prof. K. Laasonen
Department of Chemistry, School of Chemical Technology
Aalto University
P.O. Box 16100, FI-00076 Aalto (Finland)
E-mail: kari.laasonen@aalto.fi
O. Reynaud, Prof. A. G. Nasibulin, Dr. J. Sainio, Dr. H. Jiang, Prof. E. I. Kauppinen
Department of Applied Physics, School of Science
Aalto University
P.O. Box 15100, FI 00076 Aalto (Finland)
Prof. A. G. Nasibulin
Skolkovo Institute of Science and Technology
100 Novaya st., Skolkovo, 143025 (Russia)
Prof. K. Laasonen
COMP Centre of Excellence in Computational Nanoscience
Aalto University
P.O. Box 11100, FI-00076 Aalto (Finland)

[**] This work is supported by Aalto University (MOPPI project in AEF program). It was also partially supported by the Ministry of Education and Science of Russian Federation (Project DOI: RFMEFI58114X0006). This work made use of the Aalto University Nanomicroscopy Center (Aalto-NMC) premises.

Supporting information for this article is available on the WWW under http://dx.doi.org/10.1002/anie.201411450.

implies a fast procedure for producing CNT-supported catalyst.

The SCEIN/SWNT sample was grown using a one-step so-called floating catalyst (aerosol) CVD synthesis process described elsewhere.[15c] An aerosolized feedstock solution of ferrocene and thiophene in toluene was introduced into a high-temperature reactor to produce Fe catalyst nanoparticles. Ethylene (C_2H_4) was utilized as a carbon source for the CNT synthesis because hydrocarbons have shown a high reaction yield, which is a key factor for industrial applications (Figure S1). Carbon dioxide was used as an etching agent that can remove amorphous carbon coated on the surfaces of iron catalyst nanoparticles. It can also prevent the formation of cementite (Fe_3C) which is believed to be an inactive phase for the growth of nanotubes.[16] This method for the growth of CNTs has recently been described to fabricate highly conductive and transparent films.[15c]

After the synthesis, the product was studied by high-resolution transmission electron microscopy (HRTEM). This observation (Figures 1 a–c and S2) indicates SCEINs with a size distribution of 2–3 nm on the sidewalls of the SWNTs. Single-layer carbon shells around Fe nanoparticles are clearly observed in Figure 1 b and c. A schematic representation of the structure of the SCEIN/SWNT determined from the HRTEM images is shown in Figure 1 d. An HRTEM image of SCEINs (Figure 1 b inset) shows lattice fringes with a d-spacing of 0.21 nm corresponding to the (110) reflection of iron. Size distribution analysis of the iron nanoparticles in SCEINs and diameter distribution of SWNTs in the SCEIN/SWNT material were performed by measuring 200 individual nanoparticles and 100 CNTs, respectively, from the HRTEM images (Figure S3). This analysis resulted in an average size of 2.6 nm for the iron nanoparticles in SCEINs and an average diameter of 1.7 nm for SWNTs in the SWNT/SCEIN material.

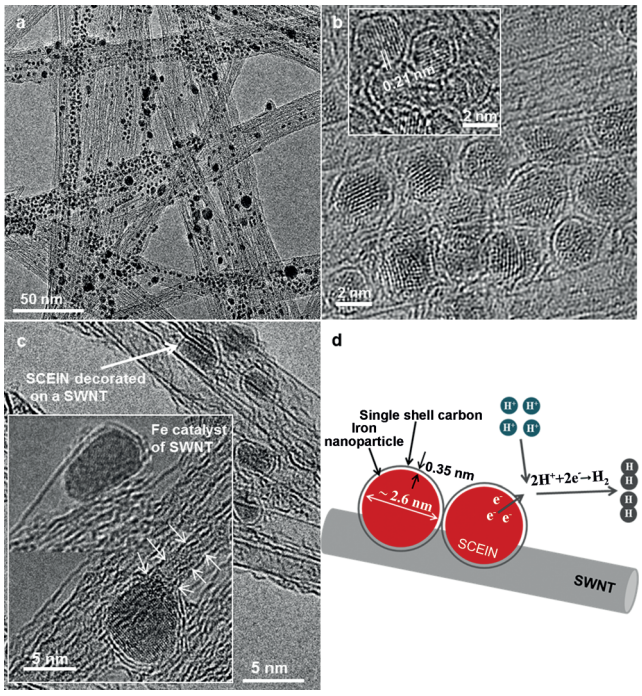

Figure 1. a) TEM image of single-shell carbon-encapsulated iron nanoparticles (SCEINs) supported on SWNTs showing distribution of the particles on the SWNTs. b) HRTEM image of the SCEIN/SWNT sample, the inset indicates the (110) lattice plane of the Fe particles in SCEINs (scale bars = 2 nm). c) HRTEM image of SCEINs decorated on the sidewalls of the SWNTs, the inset shows Fe catalyst particles for the growth of the SWNTs (arrows demonstrate the SWNT). d) Schematic representation of SCEIN/SWNT sample simplifying the HRTEM images and HER on SCEINs.

A low-magnification scanning electron microscopy (SEM) image and an energy-dispersive X-ray spectroscopy (EDS) spectrum taken from the whole area of the measured SCEIN/SWNT electrode confirmed that no noble metal was present (Figure S4). X-ray photoelectron spectroscopy (XPS) of the SCEIN/SWNT material (Figure S5) showed two peaks at binding energies of about 707 and 720 eV, which were ascribed to the metallic Fe $2p_{3/2}$ and Fe $2p_{1/2}$ peaks, respectively.[17] The absence of iron oxides in the XPS results supports the observation that the iron nanoparticles were completely covered by a carbon shell protecting them from oxidation in air. The Fe content is estimated from the XPS analysis to be 5.6 wt%; however, the encapsulation and clustering of the iron particles may cause an underestimation of the bulk amount of Fe in the SCEIN/SWNT sample.[18] The Raman spectrum of the product (Figure S6) demonstrates radial breathing modes (RBM) corresponding to SWNTs and an I_G/I_D ratio of 14.7 (detailed information provided in the Supporting Information, SI).

In our experiments for aerosol synthesis of CNTs, the TEM observations showed that iron nanoparticles with an average size of 2.6 nm are mostly inactive for the growth of CNTs and they are preferentially encapsulated with a layer of carbon, instead of growing CNTs. Figure 1 c displays the small SCEINs decorated on the sidewall of SWNTs and the Fe catalyst particles of the CNTs. In the presence of etching agents, such as CO_2, the smaller particles have less probability to serve as a catalyst for the growth of CNTs as described in our previous paper.[16a] Small particles (in our case they are 2–3 nm in diameter) have higher curvature and require small graphitic cap for the nucleation of carbon nanotube. On the contrary, the larger particles catalyze larger nucleation embryos, which have higher probability to survive in the harsh oxidizing conditions. Therefore, the larger particles may catalyze the growth of carbon nanotubes, whereas small particles are encapsulated by carbon (Figure 1 c). The latter occurs in the cooling zone of the reactor, due to the decrease in carbon solubility and etching reaction rate. In the literature, inactive iron nanoparticles have been reported during growth of CNTs as impurities which are oxidized or covered by multilayer graphene or amorphous carbon.[17,19] In contrast, we presented here a method in which those inactive Fe catalyst particles for the growth of CNTs can actually be used to synthesize SCEINs.

The catalytic activity of the SCEIN/SWNT sample for the HER was evaluated using a standard three-electrode electrochemical configuration in 0.5 M H_2SO_4 purged with N_2. As a reference, commercial Pt catalyst (20 wt% Pt/C) was also measured. All the measured catalysts were deposited on a glassy carbon electrode with a similar loading of 0.18 mg cm^{-2}. Figure 2 a shows typical polarization curves of

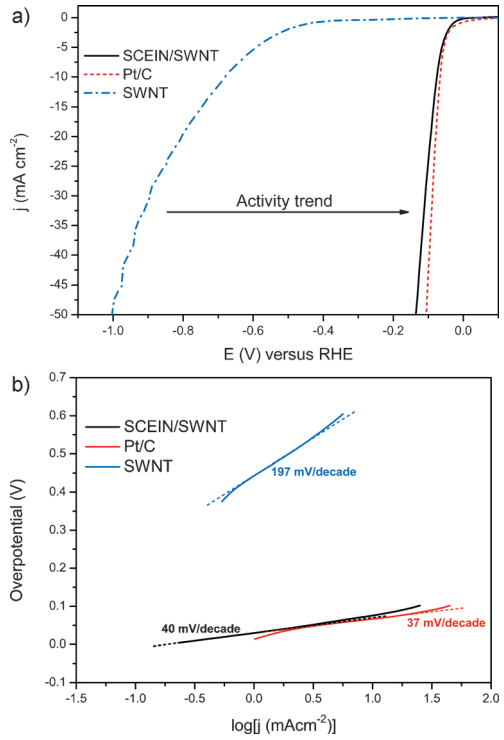

Figure 2. a) The polarization curves and b) corresponding Tafel plots of SWNT (blue), SCEIN/SWNT (black), and Pt/C (red). The polarization curves were measured at a scan rate of 50 mV s^{-1} in 0.5 M H_2SO_4 acidic solution.

HER on the pristine SWNT, SCEIN/SWNT, and Pt/C electrodes. The SCEIN/SWNT material exhibited an onset potential of about 0 V versus the reversible hydrogen electrode (RHE) which is very close to the thermodynamic potential of HER (i.e., 0 V). This onset potential is similar in magnitude to that of platinum and notably lower than that of SWNT (≈ -0.4 V), suggesting a high HER activity of SCEINs. SCEIN/SWNT resulted in a Tafel slope of 40 mV/decade ($\eta = 0$–48 mV) compared to Tafel slopes of 37 and 197 mV/decade for Pt/C and SWNT, respectively. The low Tafel slope of 40 mV/decade for SCEIN/SWNT showed that this material catalyzes the HER through a Volmer–Heyrovsky mechanism in which a fast discharge step (Volmer reaction, $H_3O^+ + e^- \rightarrow H_{ads} + H_2O$) is followed by an electrochemical desorption step (Heyrovsky reaction, $H_{ads} + H_3O^+ + e^- \rightarrow H_2 + H_2O$) and the desorption of hydrogen is the rate limiting step.[5b–d,20] The HER exchange current density (j_0) for SCEIN/SWNT and Pt/C, calculated from the Tafel plots by extrapolation method, are 0.19 and 0.17 mA cm^{-2}, respectively, which are clearly higher than that of SWNT (5.6×10^{-3} mA cm^{-2}). Most importantly, the exchange current density and the onset potential are of the same magnitude or even better for SCEIN/SWNT than for the commercial Pt/C catalyst. Moreover, SCEIN/SWNT requires low overpotentials of 42, 77, and 135 mV to achieve current densities of 2, 10, and 50 mA cm^{-2}, respectively. In comparison to the most active nonprecious-metal catalysts for HER, SCEIN/SWNT demonstrates very promising electrocatalytic activity toward HER in acidic media (Table S1). Hence, SCEIN/SWNT introduces a novel nonprecious catalyst for HER with an activity that rivals platinum in acidic media.

A stability test of the SCEIN/SWNT catalyst was performed by cycling the potential between −0.15 and 0.15 V (vs. RHE) in 0.5 M H_2SO_4 at a scan rate of 100 mV s^{-1}. This method of stability measurement was selected according to the previous accelerated HER testing.[4–5,7,21] The lower limit (−0.15 V) corresponds roughly to a current density of about 50 mA cm^{-2}. Figure 3a shows the HER polarization curves

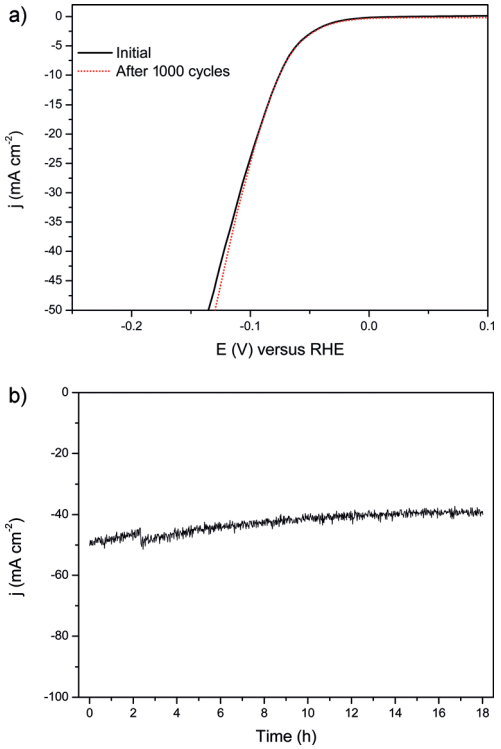

Figure 3. a) The polarization curves of SCEIN/SWNT before cycling durability test (black) and after 1000 cycles (red) between the potentials of −0.15 and 0.15 V (vs. RHE) in 0.5 M H_2SO_4 at a scan rate of 100 mV s^{-1}. b) Time dependence of the current density obtained for SCEIN/SWNT at a static potential of −135 mV for 18 h in 0.5 M H_2SO_4.

for the SCEIN/SWNT before and after 1000 potential cycles. There was no observable degradation in HER activity after this measurement, indicating that SCEIN/SWNT is a stable catalyst for HER. Time dependence of the current density for SCEIN/SWNT at a static overpotential of 135 mV was monitored for 18 h (Figure 3b). The loss in current density was smaller than that for Pt/C[5e] indicating slower poisoning, and rather similar to that of MoO_2@N-doped MoS_2 catalyst for which an approximately similar current density (≈ 50 mA cm^{-2}) was reported[5e].

In summary, SWNT-supported iron nanoparticles have been encapsulated in a carbon shell through a novel fast and low-cost one-step CVD synthesis. The encapsulation of the active transition metals, such as iron nanoparticles, in a single-layer carbon cage is proposed as a promising method to protect the active metal nanoparticles from oxidation while the desired access of the reactants to the vicinity of the metal is not prevented. The SCEIN/SWNT has been shown to be

a highly active and durable nonprecious catalyst for HER in an acidic electrolyte. The catalytic properties of this material demonstrate an inexpensive acid-stable electrocatalyst for HER with a high activity comparable to that of the best precious-metal catalysts such as platinum and superior to the best nonprecious catalysts available today. This is the first time that a method for the synthesis of metal nanoparticles encapsulated in a single-layer carbon cage is reported. This work introduces a new catalyst for HER and opens new avenues for the growth of encapsulated metal nanoparticles which can be used in various applications.

Keywords: carbon nanotubes · electrocatalysis · hydrogen evolution reaction · iron nanoparticles · nonprecious metal catalysts

How to cite: *Angew. Chem. Int. Ed.* **2015**, *54*, 4535–4538
Angew. Chem. **2015**, *127*, 4618–4621

[1] J. A. Turner, *Science* **2004**, *305*, 972–974.
[2] T. R. Cook, D. K. Dogutan, S. Y. Reece, Y. Surendranath, T. S. Teets, D. G. Nocera, *Chem. Rev.* **2010**, *110*, 6474–6502.
[3] a) E. S. Andreiadis, P.-A. Jacques, P. D. Tran, A. Leyris, M. Chavarot-Kerlidou, B. Jousselme, M. Matheron, J. Pécaut, S. Palacin, M. Fontecave, V. Artero, *Nat. Chem.* **2013**, *5*, 48–53; b) H. B. Gray, *Nat. Chem.* **2009**, *1*, 7–7.
[4] Q. Liu, J. Tian, W. Cui, P. Jiang, N. Cheng, A. M. Asiri, X. Sun, *Angew. Chem. Int. Ed.* **2014**, *53*, 6710–6714; *Angew. Chem.* **2014**, *126*, 6828–6832.
[5] a) W.-F. Chen, K. Sasaki, C. Ma, A. I. Frenkel, N. Marinkovic, J. T. Muckerman, Y. Zhu, R. R. Adzic, *Angew. Chem. Int. Ed.* **2012**, *51*, 6131–6135; *Angew. Chem.* **2012**, *124*, 6235–6239; b) J. Kibsgaard, T. F. Jaramillo, F. Besenbacher, *Nat. Chem.* **2014**, *6*, 248–253; c) Y. Li, H. Wang, L. Xie, Y. Liang, G. Hong, H. Dai, *J. Am. Chem. Soc.* **2011**, *133*, 7296–7299; d) Z. Chen, D. Cummins, B. N. Reinecke, E. Clark, M. K. Sunkara, T. F. Jaramillo, *Nano Lett.* **2011**, *11*, 4168–4175; e) W. Zhou, D. Hou, Y. Sang, S. Yao, J. Zhou, G. Li, L. Li, H. Liu, S. Chen, *J. Mater. Chem. A* **2014**, *2*, 11358–11364; f) D. H. Youn, S. Han, J. Y. Kim, J. Y. Kim, H. Park, S. H. Choi, J. S. Lee, *ACS Nano* **2014**, *8*, 5164–5173; g) D. Voiry, H. Yamaguchi, J. Li, R. Silva, D. C. B. Alves, T. Fujita, M. Chen, T. Asefa, V. B. Shenoy, G. Eda, M. Chhowalla, *Nat. Mater.* **2013**, *12*, 850–855; h) C. Wan, Y. N. Regmi, B. M. Leonard, *Angew. Chem. Int. Ed.* **2014**, *53*, 6407–6410; *Angew. Chem.* **2014**, *126*, 6525–6528.
[6] X. Zou, X. Huang, A. Goswami, R. Silva, B. R. Sathe, E. Mikmeková, T. Asefa, *Angew. Chem. Int. Ed.* **2014**, *53*, 4372–4376; *Angew. Chem.* **2014**, *126*, 4461–4465.
[7] E. J. Popczun, J. R. McKone, C. G. Read, A. J. Biacchi, A. M. Wiltrout, N. S. Lewis, R. E. Schaak, *J. Am. Chem. Soc.* **2013**, *135*, 9267–9270.
[8] J. Deng, P. Ren, D. Deng, L. Yu, F. Yang, X. Bao, *Energy Environ. Sci.* **2014**, *7*, 1919–1923.
[9] Z. Zhang, B. Lu, J. Hao, W. Yang, J. Tang, *Chem. Commun.* **2014**, *50*, 11554–11557.
[10] Y. Zheng, Y. Jiao, Y. Zhu, L. H. Li, Y. Han, Y. Chen, A. Du, M. Jaroniec, S. Z. Qiao, *Nat. Commun.* **2014**, *5*, 3783.
[11] Y. Zheng, Y. Jiao, L. H. Li, T. Xing, Y. Chen, M. Jaroniec, S. Z. Qiao, *ACS Nano* **2014**, *8*, 5290–5296.
[12] a) G. Wu, K. L. More, C. M. Johnston, P. Zelenay, *Science* **2011**, *332*, 443–447; b) H. T. Chung, J. H. Won, P. Zelenay, *Nat. Commun.* **2013**, *4*, 1922; c) D. Deng, L. Yu, X. Chen, G. Wang, L. Jin, X. Pan, J. Deng, G. Sun, X. Bao, *Angew. Chem. Int. Ed.* **2013**, *52*, 371–375; *Angew. Chem.* **2013**, *125*, 389–393.
[13] Y. Hu, J. O. Jensen, W. Zhang, L. N. Cleemann, W. Xing, N. J. Bjerrum, Q. Li, *Angew. Chem. Int. Ed.* **2014**, *53*, 3675–3679; *Angew. Chem.* **2014**, *126*, 3749–3753.
[14] S. Taubert, K. Laasonen, *Phys. Chem. Chem. Phys.* **2014**, *16*, 3648–3660.
[15] a) G. G. Wildgoose, C. E. Banks, R. G. Compton, *Small* **2006**, *2*, 182–193; b) W. Zhang, P. Sherrell, A. I. Minett, J. M. Razal, J. Chen, *Energy Environ. Sci.* **2010**, *3*, 1286–1293; c) O. Reynaud, A. G. Nasibulin, A. S. Anisimov, I. V. Anoshkin, H. Jiang, E. I. Kauppinen, *Chem. Eng. J.* **2014**, *255*, 134–140.
[16] a) Y. Tian, M. Timmermans, S. Kivistö, A. Nasibulin, Z. Zhu, H. Jiang, O. Okhotnikov, E. Kauppinen, *Nano Res.* **2011**, *4*, 807–815; b) A. G. Nasibulin, A. S. Anisimov, P. V. Pikhitsa, H. Jiang, D. P. Brown, M. Choi, E. I. Kauppinen, *Chem. Phys. Lett.* **2007**, *446*, 109–114; c) P. R. Mudimela, A. G. Nasibulin, H. Jiang, T. Susi, D. Chassaing, E. I. Kauppinen, *J. Phys. Chem. C* **2009**, *113*, 2212–2218.
[17] C.-M. Yang, H. Kanoh, K. Kaneko, M. Yudasaka, S. Iijima, *J. Phys. Chem. B* **2002**, *106*, 8994–8999.
[18] C. He, S. Wu, N. Zhao, C. Shi, E. Liu, J. Li, *ACS Nano* **2013**, *7*, 4459–4469.
[19] a) H.-T. Fang, C.-G. Liu, C. Liu, F. Li, M. Liu, H.-M. Cheng, *Chem. Mater.* **2004**, *16*, 5744–5750; b) G. Zhou, D.-W. Wang, P.-X. Hou, W. Li, N. Li, C. Liu, F. Li, H.-M. Cheng, *J. Mater. Chem.* **2012**, *22*, 17942–17946.
[20] a) B. E. Conway, B. V. Tilak, *Electrochim. Acta* **2002**, *47*, 3571–3594; b) W. F. Chen, C. H. Wang, K. Sasaki, N. Marinkovic, W. Xu, J. T. Muckerman, Y. Zhu, R. R. Adzic, *Energy Environ. Sci.* **2013**, *6*, 943–951.
[21] T. Wang, L. Liu, Z. Zhu, P. Papakonstantinou, J. Hu, H. Liu, M. Li, *Energy Environ. Sci.* **2013**, *6*, 625–633.

Received: November 26, 2014
Published online: February 12, 2015

